Radiation Physics and Chemistry 245 (2026) 113884

Contents lists available at ScienceDirect

Radiation Physics and Chemistry

journal homepage: www.elsevier.com/locate/radphyschem

Production of negatively charged atomic ions inside a linear Paul trap for the formation of antiprotonic atoms

Ł. Kłosowski [a], M. Piwiński [a,*], A. Linek [a], M. Grosbart [b], R. Ciuryło [a], M. Zawada [a], M. Teske [c], T. Sowiński [c], S. Alfaro Campos [d,e], M. Auzins [f], D. Bhanushali [d], A. Bhartia [d,g], M. Berghold [h], R.S. Brusa [i,j], K. Calik [b], A. Camper [k], R. Caravita [j], F. Castelli [l,m], G. Cerchiari [d,e], S. Chandran [n,w], A. Chehaimi [i,j], S. Choudapurkar [d], P. Conte [l,m], G. Consolati [l,o], M. Doser [p], R. Ferguson [i,j], M. Germann [p], A. Giszczak [b], L.T. Glöggler [p], Ł. Graczykowski [b], F. Guatieri [h,i,j], N. Gusakova [p,q], F.P. Gustafsson [p], S. Haider [p], S. Huck [p,r], C. Hugenschmidt [h], M. Jakubowska [b], M.A. Janik [b], G. Kasprowicz [s], K. Kempny [b], G. Khatri [p], A. Kisiel [b], G. Kornakov [b], V. Krumins [f,p], L. Lappo [b], S. Mariazzi [i,j], P. Moskal [t,u], M. Münster [h], P. Pandey [t,u], D. Pecak [c], L. Penasa [i,j], F. Prelz [l], T. Rauschendorfer [p,v], B.S. Rawat [n,w], B. Rienäcker [n], V. Rodin [p], H. Sandaker [k], S. Sharma [t,u], E. Teberga [f], M. Tockner [d], M. Volponi [p], C.P. Welsch [n,w], J. Zieliński [b], N. Zurlo [x,y]

[a] Institute of Physics, Faculty of Physics, Astronomy and Informatics, Nicolaus Copernicus University in Toruń, Grudziadzka 5, 87-100 Toruń, Poland
[b] Warsaw University of Technology, Faculty of Physics, ul. Koszykowa 75, 00-662, Warsaw, Poland
[c] Institute of Physics, Polish Academy of Sciences, Aleja Lotnikow 32/46, PL-02668 Warsaw, Poland
[d] University of Siegen, Department of Physics, Walter-Flex-Strasse 3, 57072 Siegen, Germany
[e] Universität Innsbruck, Institut für Experimentalphysik, Technikerstrasse 25/4, 6020 Innsbruck, Austria
[f] University of Latvia, Department of Physics, Raina boulevard 19, LV-1586, Riga, Latvia
[g] Université de Genéve, 24 rue du Général-Dufour, 1211 Genéve 4, Switzerland
[h] Heinz Maier Leibnitz Zentrum (MLZ), Technical University of Munich, Lichtenbergstraße 1, 85748, Garching, Germany
[i] Department of Physics, University of Trento, via Sommarive 14, 38123 Povo, Trento, Italy
[j] TIFPA/INFN Trento, via Sommarive 14, 38123 Povo, Trento, Italy
[k] Department of Physics, University of Oslo, Sem Sælandsvei 24, 0371 Oslo, Norway
[l] INFN Milano, via Celoria 16, 20133 Milano, Italy
[m] Department of Physics "Aldo Pontremoli", University of Milano, via Celoria 16, 20133 Milano, Italy
[n] Department of Physics, University of Liverpool, Liverpool L69 3BX, UK
[o] Department of Aerospace Science and Technology, Politecnico di Milano, via La Masa 34, 20156 Milano, Italy
[p] CERN, 1211 Geneva 23, Switzerland
[q] Department of Physics, NTNU, Norwegian University of Science and Technology, Trondheim, Norway
[r] Institute for Experimental Physics, Universität Hamburg, 22607, Hamburg, Germany
[s] Warsaw University of Technology, Faculty of Electronics and Information Technology, ul. Nowowiejska 15/19, 00-665 Warsaw, Poland
[t] Marian Smoluchowski Institute of Physics, Jagiellonian University, ul. Łojasiewicza 11, 30-348 Kraków, Poland
[u] Centre for Theranostics, Jagiellonian University, ul. Kopernika 40, 31-501 Kraków, Poland
[v] Felix Bloch Institute for Solid State Physics, Universität Leipzig, 04103 Leipzig, Germany
[w] The Cockcroft Institute, Daresbury, Warrington WA4 4AD, UK
[x] INFN Pavia, via Bassi 6, 27100 Pavia, Italy
[y] Department of Civil, Environmental, Architectural Engineering and Mathematics, University of Brescia, via Branze 43, 25123 Brescia, Italy

ARTICLE INFO

Keywords:
Anions
Ion traps
Ion beams

ABSTRACT

An effective, long-lasting, low-energy source of negatively charged ions was designed, constructed, and tested. The source uses electron dissociative attachment in electron-molecule collisions to form a set of anions inside a linear Paul trap. Iodine I_2 molecules were used to obtain pure sets of I^- anions. The system was tested,

* Corresponding author.
E-mail addresses: lklos@fizyka.umk.pl (Ł Kłosowski), Mariusz.Piwinski@fizyka.umk.pl (M. Piwiński).

https://doi.org/10.1016/j.radphyschem.2026.113884
Received 27 November 2025; Accepted 29 March 2026
Available online 31 March 2026

Electron dissociative attachment
Iodine

providing about 10^5 ions produced in less than a minute, which can be stored in the trap and used in further experiments.

1. Introduction

The majority of experiments involving trapped ions use positively charged ions (cations) as the object of interest. Lack of an electron in their structure makes them relatively stable objects, which may be applied in numerous experimental studies, including long-time preservation of their quantum states, like in quantum simulations, quantum information processing, quantum metrology, etc. They are usually well-described quantum systems allowing to manipulate them optically using precise laser systems.

On the other hand, negatively charged ions (anions) do not possess such advantages. Most of them have only one electronic bound state, making them impossible to be controlled optically. Atoms typically have relatively low electron affinity, which makes the negatively charged ions much more vulnerable to destruction than positive ones. For these reasons, anions have not been widely used in experiments, however in some experimental studies, they may be necessary to be advantageously used instead of cations.

An example of such a situation are matter-antimatter interaction studies, where antiprotons having a negative electric charge are involved. To provide long-time co-trapping them with other objects, such partners should be negatively charged as well. In further steps, such ions can be used for production of antiprotonic atoms — systems where one of the electrons is substituted with an antiproton (Hartmann, 2000; Andersen, 2004).

There are numerous studies on trapped anions, involving molecules such as C_2^-, OH^-, or more complex ones (Otto et al., 2013; Lakhmanskaya et al., 2020; Mant et al., 2020; Cerchiari et al., 2019; Deiglmayr et al., 2012). There are also known sources of atomic anions. They were broadly discussed in a recent review by Bacal et al. (2021). The most universal, by the means of variety of species produced, is Middleton's source (Middleton, 1983), which uses optical ablation of a solid with occasional production of anions in the created plasmas. However, such devices provide a mixed ensemble of anions. Additionally, they can only serve for a relatively short time due to depletion. Long lasting hydrogen anion H^- sources are used by particle accelerators, such as Linac4 at CERN, to provide ions as an intermediate step to produce intense protonic beams (Vretenar et al., 2020).

The goal of this work was to construct a long-lasting, stable, repetitive, controllable source of low-energy atomic anions. Additionally, the source should have a compact geometry, so it could be easily attached to larger experimental apparatuses. In particular, the source is intended to cooperate with the AEgIS apparatus at CERN https://aegis.web.cern.ch/.

2. Considerations on production of ions

The controlled process of removing an electron from an atom to create a cation is a relatively easy task. It can be performed via photoionization (Kjaergaard et al., 2000; Gulde et al., 2001) or ionization in collisions with particles like electrons (Kłosowski et al., 2018). Such methods were widely studied and are well-known and commonly used techniques (Major et al., 2005; Werth et al., 2009).

In contrast, attaching an excessive electron to form an anion may be significantly more challenging. Attaching of an electron to an atom in a single two-body collision is not possible since there is no simple mechanism to dissipate the excess energy of the collision partners. To overcome this issue, one needs to utilize a three-body collision. Here, the third partner carries away the excessive energy after the collision. This would require a dense gas environment, increasing the probability of such collisions, which is however in contradiction to vacuum conditions, as usually required in experiments.

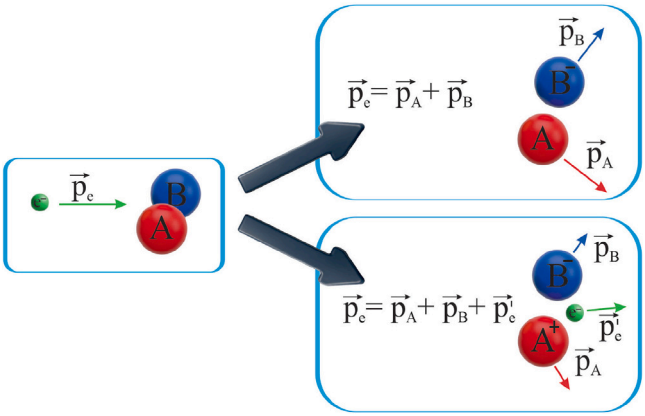

Fig. 1. An illustration of possible dissociation channels of a molecule bombarded with an electron, forming a negatively charged ion.

Fortunately, there is another possibility An alternative to involve effectively a third partner to a collision is provided by the use of molecular targets instead of atomic ones. In a well-known process of electron dissociative attachment (Fabrikant et al., 2017), a molecule bombarded with electrons can split into two or more fragments, some of which may be negatively charged. In some cases, such dissociation can be enhanced by resonant effects (Bardsley and Mandl, 1968). It happens when in the intermediate state, an electron is temporarily attached to a molecule, forming a short-lived (femtoseconds) anion. Such an ion can dissociate into fragments of various charges. In general, such formation of anions can be realized in one of the following schemes (illustrated in Fig. 1):

$$AB + e \longrightarrow A + B^- \tag{1}$$

$$AB + e \longrightarrow A^+ + B^- + e \tag{2}$$

Since a molecule can dissociate in various channels (also with more than two fragments), the resulting ensemble of ions may contain different species. The number of possible channels depends on the molecule's structure. To obtain a pure ensemble of anions of one species, one should use a diatomic, homonuclear molecule.

The best choice are diatomic molecules of halogens. Their atoms have the highest values of electron affinity, leading to high stability of the resulting anions. In our work iodine was chosen as a test target. It is solid at room temperature, which makes it relatively easy to handle. Also the natural isotope composition of iodine contains only one nuclide, ^{127}I, providing an expected pure set of just one type of anions.

The iodine, when bombarded with electrons, may dissociate in several channels, two of them providing atomic anions:

$$I_2 + e \longrightarrow I^- + I \tag{3}$$

$$I_2 + e \longrightarrow I^- + I^+ + e \tag{4}$$

The energy threshold for the process (3) is 0, while for the process (4) it is 8.93 eV. These numbers can be determined as follows: the electron affinity of iodine is 3.06 eV (Pelaez et al., 2009), the first ionization energy of iodine atom is 10.45 eV (Esteves et al., 2023), and the dissociation energy of an iodine molecule is 1.54 eV (Barrow et al., 1973). Since the affinity has a larger value than the dissociation energy, any electron can cause the dissociation. The threshold for the process

(4) is the ionization energy plus dissociation energy minus the electron affinity.

In the first case, the output energy will be almost equally shared by both fragments, which is a consequence of the linear momentum conservation principle. In the second case, the energy and the linear momentum are shared by three particles, so some of the ions in the obtained ensemble may be colder than the ones produced in the first process.

Unfortunately, up to now, only few experiments on electron collisions with iodine have been performed, and the available data sets on cross sections for both processes are very limited (Frost and McDowell, 1960). This may be due to the fact that iodine is a very strong oxidizer, causing corrosion even to stainless steel elements, which makes the experimental work with the element very challenging. Available theoretical datasets are also very limited (Zatsarinny et al., 2011; Yadav et al., 2020).

2.1. Iodine-induced corrosion risk and use of iodoform as a safe target

To check the corrosive properties of iodine, we performed a series of tests with iodine and 316 stainless steel. In the first test, we put a piece of steel in a tight glass container together with a piece of iodine. Since the iodine evaporates very efficiently, the contact of the steel with iodine was well established. We left the pieces in the container for five days, at room temperature and with the air inside. The surface of the material became strongly corroded, therefore any steel element of a vacuum apparatus would be damaged after several days of contact with the iodine vapor.

The second attempt was putting the steel fragments in a small, steel vacuum tube. The tube was pumped down the to the vacuum level well below the iodine's vapor pressure (about 0.2 mbar at room temperature (Stull, 1947)) and left for five days. In this test, we examined the steel surface very carefully and no visible trace of corrosion was observed. Any possible contamination was too small to be noticed by eye and may be considered negligible. This leads to the conclusion that for oxidation of the steel the presence of air is necessary. Possibly, the air humidity may play a role in the process. These tests show that working with molecular iodine may be safe, if sufficient vacuum conditions are maintained. Moreover, the predicted use of iodine in the experiment is of the order of micrograms per day, which, combined with low steel oxidation rate, should provide good operation conditions for the apparatus for a long time.

At the testing stage of the proposed method, we decided to use temporarily another molecule — iodoform CHI_3. Its physical properties are similar to that of iodine, but it is much less active chemically. It may dissociate in more channels, some of them providing negatively charged elemental ions:

$$CHI_3 + e \longrightarrow CHI_2 + I^- \tag{5}$$

$$CHI_3 + e \longrightarrow CHI + I + I^- \tag{6}$$

$$CHI_3 + e \longrightarrow CH + I_2 + I^- \tag{7}$$

$$CHI_3 + e \longrightarrow CH + 2I + I^- \tag{8}$$

It should be noted that in the case of iodoform, the resulting ensemble of anions would not be pure but would contain I^-, CI^-, CHI^-, etc.

3. Anion production rates at given conditions

The idea of the experiment is to produce a set of anions by bombarding iodine/iodoform molecules with electrons at energies of several tens of eV. The resulting ions are collected in a linear Paul trap. Finally, sufficiently large ensembles of ions can be ejected from the trap in a single pulse towards the main part of the experiment, where antiprotonic atoms will be later formed. Thus, it is important to estimate the anion production rates.

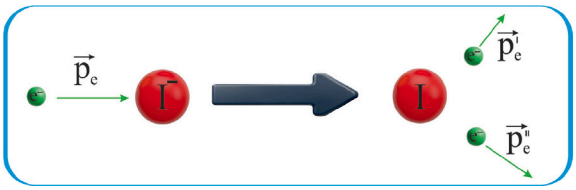

Fig. 2. An illustration of neutralization of an anion via electron collision.

Assuming that we can estimate the electron beam current I and energy E, the anion formation cross section σ (which depends on the energy), the number density of iodine n and the effective size of electron-molecule interaction region l, the production rate of anions is given by the expression:

$$\dot{N} = \frac{I}{e} nl\sigma(E) \tag{9}$$

where e denotes the elementary charge. Assuming: $I = 10^{-6}$ A (typical for the electron gun used in the experiment), $n = 10^{14}$ m^{-3} (density at 10^{-8} mbar and room temperature), $l = 10^{-3}$ m, $\sigma = 10^{-21}$ m^2 (typical order of magnitude for electron collision processes), one may expect $\dot{N} = 1000$ s^{-1}. Such rates can allow to prepare a set of a million ions in a few minutes of loading of the trapping system.

3.1. Anion loss rates

The anions are lost from the trapping system in several possible processes:

1. Evaporation: the trapping potential always has a finite depth, and the ions in the ensemble may have various kinetic energies, given with some distribution. The hottest ions may be lost from the trap as they may cross the trapping potential barriers. This effect provides additional evaporative cooling of the ion ensemble.
2. Electron-ion collisions, leading to ionization (neutralization) according to the equation (illustrated in Fig. 2):

   $$I^- + e \longrightarrow I + 2e \tag{10}$$

   The energy threshold for this process is equal to the electron affinity of iodine atom (3.06 eV). Since the electron energy used to load the trap is usually well above this value, such processes will be observed whenever the electron beam is present in the system.
3. Charge-transfer collisions of iodine anions with molecules of background gas, according to the equation:

   $$I^- + X \longrightarrow I + X^-, \tag{11}$$

   where X denotes any molecule present in the background gas. Depending on the molecule, the energy threshold will be of the order of few eV. Similar to the first process, this one may also lead to cooling of the ion ensemble by removing the hottest ions.

The mentioned processes lead to modification of Eq. (9) to form:

$$\dot{N} = \frac{I}{e}\left(nl\sigma(E) - \frac{N}{S}\varsigma(E)\right) - \beta N, \tag{12}$$

where ς is the cross section for electron impact neutralization of the anion, S is the effective cross section of the cloud of trapped ions, and β is the loss rate resulting from evaporation and charge-transfer collisions.

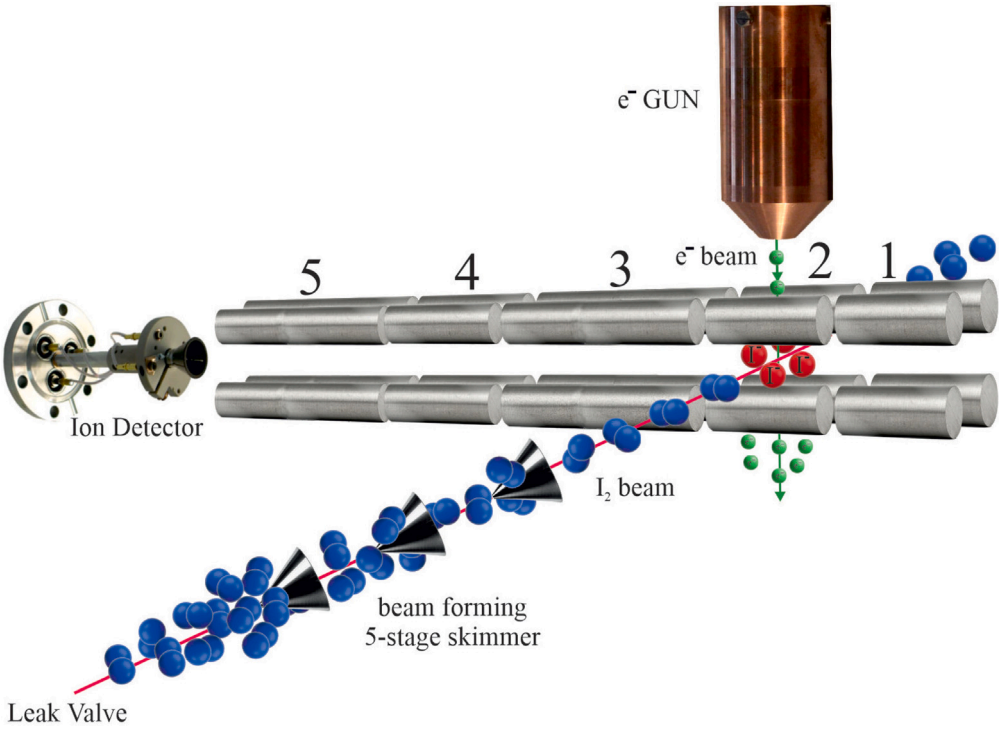

Fig. 3. Schematic of the experimental setup. The electronic and molecular beams are produced by an electron gun and a leak valve with a 5-stage skimmer. They are cross-fired in one of the segments of the linear Paul trap, where the iodine anions are created in electron-molecule collisions. The ions can be ejected towards the detector placed at the end of the trap.

The ion loss has two consequences: saturation of the ion number while loading the trap, and loss of the ions after loading is completed. Saturation is expected for N ions where:

$$N = \frac{nl\sigma(E)}{\frac{\varsigma(E)}{S} + \beta\frac{e}{I}}, \tag{13}$$

which is reached with a characteristic time of:

$$\tau = \frac{1}{\frac{I}{e}\frac{\varsigma(E)}{S} + \beta}. \tag{14}$$

Assuming the same conditions as at loading, and $S = 10^{-4}$ m^2, $\varsigma = 10^{-21}$ m^2, $\beta = 10^{-2}$ s^{-1}, one may reach the number: $N = 10^5$ in a characteristic time of 100 s.

For ion loss after loading, one must only substitute $I = 0$ to the Eqs. (13) and (14), leading to an empty trap ($N = 0$) at the final equilibrium and a slightly longer characteristic time.

It will be subsequently shown that the dynamics of production and loss of the ions determined experimentally are consistent with the above equations.

4. Cooling, manipulating and detection of the anions

Compared to cations, experiments with anions may present several serious challenges. Almost all atomic anions have only one bound state, making any optical manipulation very difficult, if not impossible. This leads to issues with cooling, manipulating, and detection of the ions.

The detection may be feasible using electronic methods (Major et al., 2005), which however has never been performed in a linear Paul trap. In the proposed experiment, we decided to use a destructive detection with a channel electron multiplier to count the ions extracted from the trap. The method may be used only as a way to test the efficiency and stability of the anion source before the actual experiment. For the proper part of the experiment, an assumption will be necessary: that the source's performance is stable and repeatable.

Cooling of the anions cannot be performed in any known optical schemes. In a very limited range, one can perform an evaporative cooling, or adiabatic cooling, or try to develop other schemes of manipulating the trapping potentials leading to energy dissipation. Some role in the cooling process may be played by collision of the anions with background gas. If the collision energy is higher than the electron affinity of the anion (about 3 eV), neutralization of the ion by electron detachment is possible. This may lead to removal of the ions with higher energies from the ensemble.

Also, if the ion was formed in the process described with Eq. (4), we may expect it to be relatively cold, so further cooling may be unnecessary.

The required final temperature of the anion ensemble is determined by the required time performance of the ion pulse. In further analysis, we found that the accelerating pulse of the potential, forming the ionic pulse, causes an energy spread of several tens of eV. This means that cooling the ions below 3 eV is pointless, so we decided not to introduce any further cooling mechanisms.

Manipulation of the ions may be achieved only via driving the trapping potentials of the trap. By appropriate choice of the potentials, one can provide different shapes, densities, and total numbers of ions in the ensemble.

5. Design of the apparatus

The experimental system is based on a linear, segmented Paul trap. It is divided into 5 segments, allowing to form two separate trapping regions. It was intended to allow storage of iodine in both the centers and performing experimental studies with just a fraction of the ion ensemble in the future. Such a design may also provide a relatively high level of flexibility in preparing various trapping potentials. The scheme of the trap is presented in Fig. 3.

The trap contains five segments, numbered as in the scheme in Fig. 3. The trapping centers may be formed inside the segments 2 and 4 (however it is not the only possible configuration). Inside the segment

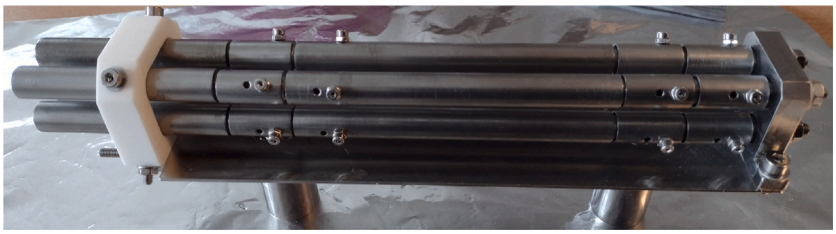

Fig. 4. Photograph of the ion trap used in the experiment, before it was installed in the vacuum chamber and wired for the voltage supplies. The electrodes are made of molybdenum, and the support frame is mostly made of stainless steel. The white supporting element is made of macor.

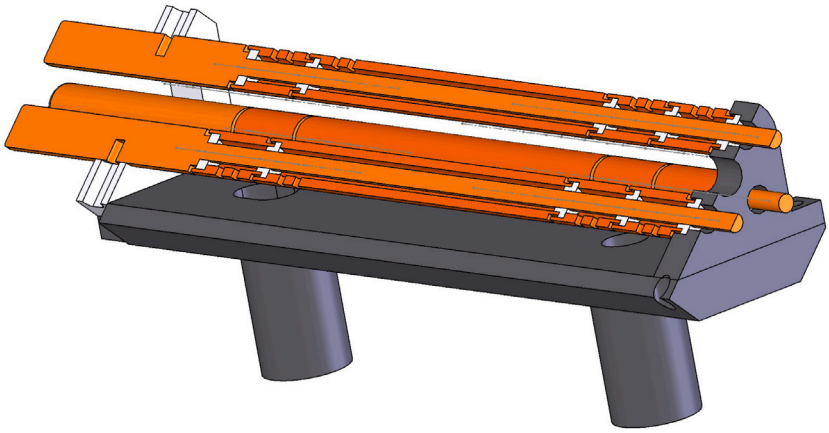

Fig. 5. A cross section of the trap (compare to the photograph presented in Fig. 4). Note that the insulating macor elements (white in the picture) that separate the electrode segments are hidden to avoid being exposed to stray electrons.

2, an electron beam and a molecular beam are cross-fired, allowing to create anions in this trapping segment.

Each segment contains 4 electrodes arranged in a quadrupole geometry, making 20 electrodes in total. One diagonal of the trap is AC+DC voltage-supplied, while the other is DC only. The electrodes are made of molybdenum, which is known for its good performance when working with electron beams (good electric and heat conduction, high stiffness). The photograph of the trap before installation in the vacuum chamber is presented in Fig. 4. The insulating elements are made of macor and designed to be hidden inside electrodes, to avoid charge patches from electrons settling on dielectric surfaces. The details are presented in Fig. 5. The diameter of a single electrode is 10 mm, with a gap of 4 mm between the electrodes. The segment lengths are 20 mm, 20 mm, 100 mm, 20 mm, and 60 mm respectively.

The voltage supply of the trap is presented in Fig. 6. It consist of an AC part, a DC part and an AC–DC mixer. The AC part consists of a function generator (Rigol DG 1022Z 25 MHz), a 50-times amplifier (Falco Systems WMA-300), and a custom-made helical resonator. The resonance frequency is about 1.2 MHz, allowing to achieve amplitudes from 0 to 800 Vpp. The DC voltages are provided by a set of computer-controlled power supplies, allowing to drive the potentials during the experiments in designed time sequences. The available voltages are in the range of ±200 V. The AC and DC voltages are mixed using a set of 5 simple RC mixers, connected in parallel, one for each segment of the trap.

The electron beam is produced by a custom-made electron gun, similar to the ones used in our previous experiments on electron impact ionization (Kłosowski et al., 2018). The scheme of the electron gun is presented in Fig. 7. It uses a hot tungsten filament as a primary source of electrons. They are accelerated to energies which can be set between several eV and several hundreds of eV, forming a beam. Typically, it is most convenient to work with electrons of energies between 50 eV and 100 eV. At lower energies, the gun efficiency may be insufficient, and for higher energies, the electrons would heat up the electrodes of the

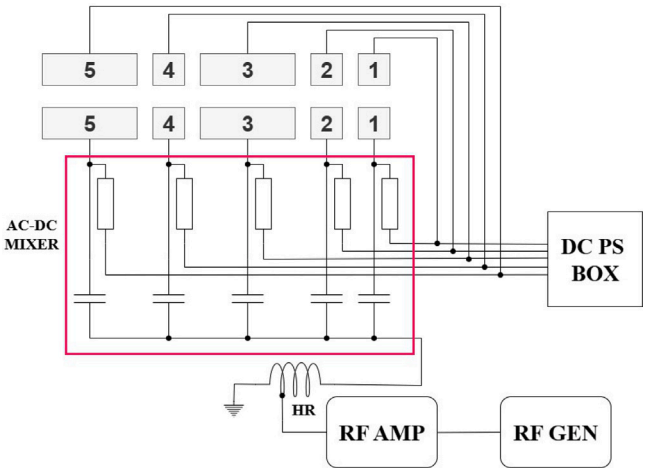

Fig. 6. Electric scheme of the voltage supply of the Paul trap. The RF potentials are provided by a system consisting of function generator (RF GEN), amplifier (RF AMP), and helical resonator (HR). The DC potentials are provided by a set of standard power supplies (DC PS BOX). Both potentials are mixed with simple RC mixers.

trap, influencing the vacuum conditions. To avoid detection of stray electrons in the experiment, the electron source may work in a pulsed mode (Kłosowski et al., 2018) by switching the potential of the Wehnelt electrode to very low values, blocking transmission of any electrons.

Since the Paul trap produces rapidly changing electric fields, the electron beam cannot be well focused or precisely directed inside the trap. This is the reason we decided not to use any directional electrodes or energy monochromators — they would be useless in this case, while simplicity of the gun construction is a serious advantage. At

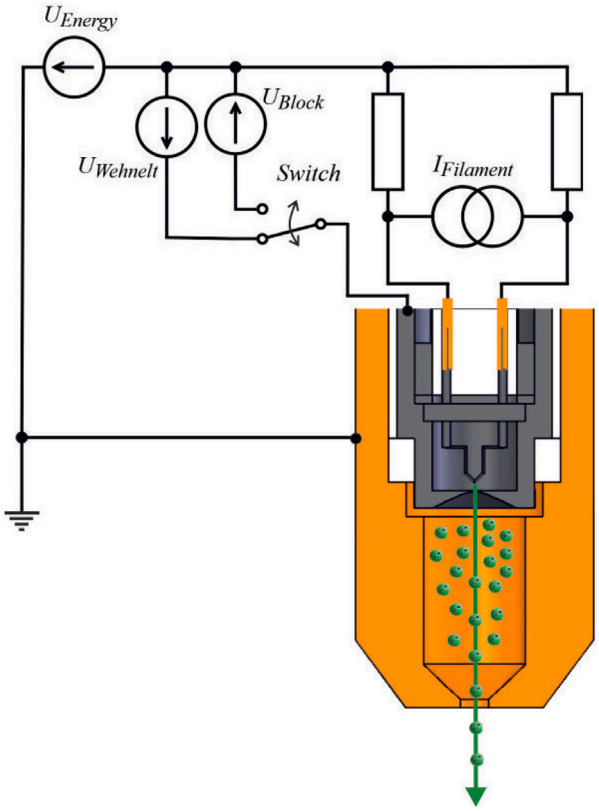

Fig. 7. Schematic of the electron gun: the electric circuit and the gun's cross section. The primary electrons are emitted from tip of a filament heated with 1.9-2.3 A current. The filament is kept on a negative potential provided by the U_{Energy} power supply, defining the electron's energy. The electrons are extracted using the Wehnelt cylinder (dark gray) and further accelerated to form a beam exiting the gun via a 2-mm orifice in the external, grounded shield (orange). The potential of the Wehnelt electrode can be switched between two values, one blocking the beam formation, and one allowing it.

regular operation of the trap, a portion of electrons would reach the trapping center anyway, providing sufficient number of collisions to form ensembles of anions.

The molecular beams are formed by a source consisting of a custom-made, temperature-controlled reservoir, a leak valve (Leybold 28990V01) and a 5-stage skimmer system. The reservoir of about 10 cubic centimeters is filled with iodine or iodoform powder (depending on the needs of a particular experiment). Both substances have a vapor pressure of the order of 1 mbar at room temperature (Stull, 1947), which is sufficient for the operation of the source without further heating or cooling. For possible future applications with other molecules, the reservoir is additionally equipped with a Peltier cooler/heater. The valve allows to drive the leak of the molecules from 10^{-10} to 10^{2} $\frac{\text{mbar l}}{\text{s}}$ at room temperature and 1 bar input pressure. The skimmers are side-pumped by a separate turbomolecular pump, so the pressure in the vacuum chamber is not affected by the iodine/iodoform molecules. The skimmers have orifices of 1 mm diameter and are separated by 30 mm gaps. This provides a beam of 1 mm diameter at the exit of the aperture and 2 mm inside the trap. To avoid scattering of stray molecules after passing the trapping region, additionally an absorber was introduced on the opposite side of the apparatus. It consists of a mesh made of silver, an efficient iodine absorber.

Both electronic and molecular beams are cross-fired in one of the centers of the trap. This way, anions can be formed according to Eqs. (3) and (4), and further stored in the trap, and later detected.

The detection system is based on a channel electron multiplier, placed on the main axis of the trap, near one of the trap's ends. The model used in the experiment is a Photonis 4230 Megaspiraltron, working in a standard pulse-counting configuration. It is a relatively universal detector, allowing to see both anions and cations, as well as electrons, and even UV photons. For the experiment, the potential of the detector's cone was set to block possible cations, allowing detection of negatively charged particles only.

The entire source is kept in vacuum conditions. The vacuum chamber was made from two 6-way crosses (Kimball Physics MCF450M-SPHSQ-E2C4), equipped with all necessary feedthroughs, gauges, etc. The vacuum is provided by a turbolecular pump (Twis Torr 305 Agilent), supported by an ion pump (Vaclon Plus 20 Agilent) (not used during the measurements due to stray electrons produced by the device). The molecular beam skimmers are pumped with a turbomolecular pump (Twis Torr 74FS Agilent). The vacuum level provided by the system is of the order of 10^{-10} mbar.

6. Experimental procedures

The experiments were performed in various configurations, allowing to characterize the source under various aspects, including the beam's performance, the trap settings, the time of loading the trap and storing the ions, etc. In general, each experimental run, after setting the beams parameters and the trapping potentials, consisted of following steps:

1. Setting a trapping minimum in the 2nd segment of the trap (maximum of the potential, since the anions are to be trapped),
2. Bombarding the molecules with electrons for a given period of time, of the order of seconds to minutes,
3. Switching off the electron beam and waiting for another period of time, also seconds to minutes,
4. Releasing the anions towards the detector by changing the trap's DC potentials to open one side of the trap,
5. Detection and counting the number of pulses, related to the number of trapped ions.

The typical measurement scheme is presented in Fig. 8. It can be noted that the kinetic energy of ions leaving the source is determined by the potential of segment 2 in relation to the ground, usually several tens or slightly above 100 eV. The ions are accelerated later by the potential of the ion detector's cone (Fig. 3) with additional 100–200 V, leading to anion energies of 100–300 eV when they hit the detector's surface. At such energies, the typical detection efficiency is a few percent.

The pulse of anions leaving the trap is slightly divergent. To estimate this divergence, a set of numerical simulations was performed. The calculations were done using custom-made software, solving the ion's equations of motion with 4th order Runge–Kutta method (John Wiley and Sons, Ltd, 2016). The simulation results suggest that about 50% of the ions would reach the detector (results of the simulations are being prepared for separate publication). Additionally, the ions reach the detector in a short pulse, so the counts from particular ions may overlap in time, as the time resolution of the channeltron system is about 100 ns. From an analysis of the time of particular pulses, it was concluded that the pulse overlap reduces the number of counts by one order of magnitude. Combined with the detector's efficiency, one may conclude that only a few percent of the ions are observed by the detector and the true number of captured ions is two orders of magnitude higher than the number of counts from the detector. The exact number is however difficult to determine, since the detector efficiency is known with large uncertainty only. In the subsequent analysis of the results, we will assume the true number of ions to be 100 times the number of counts (but could even be 10 times greater).

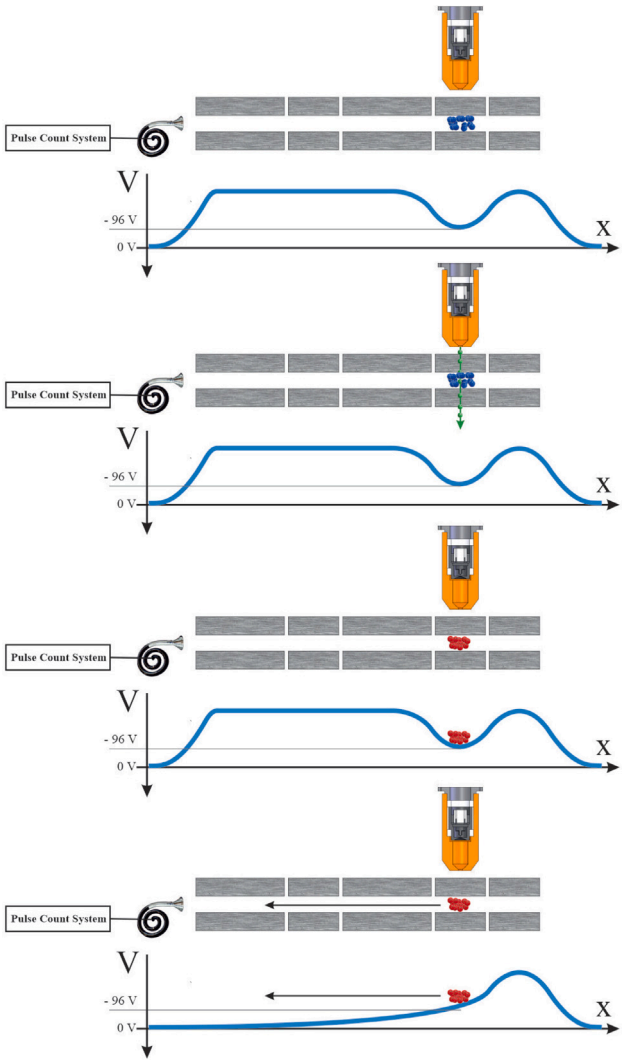

Fig. 8. Schematic of the experimental procedure. The potential axis is inverted, as we are using negatively charged particles, and such a way of presenting is more intuitive. In the first panel, a trapping minimum is formed and the molecular beam is introduced. In the second panel, the electrons bombard the molecules to form anions. In the third panel, the electron beam is turned off and the anions are stored in the trap. In the fourth panel, the anions are released towards the detector.

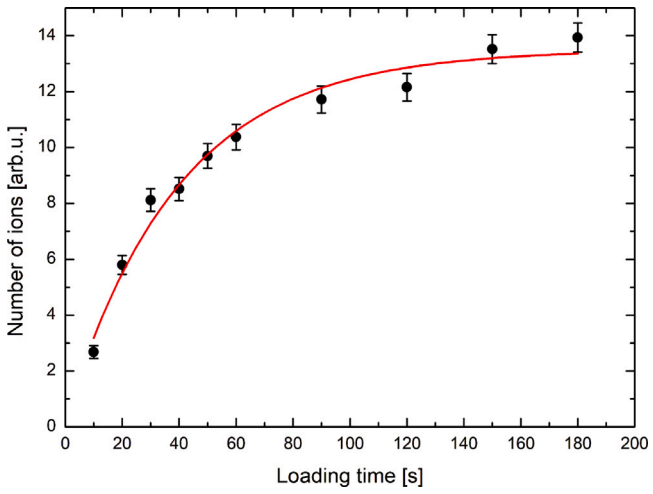

Fig. 9. Example results of a loading test of the trap. The data have been averaged from 5 separate runs. The error bars correspond to one standard deviation. The number of ions is given in arbitrary units, one unit corresponding to approximately 1000 ions. Additionally, a fitting curve is presented, see the text for the details.

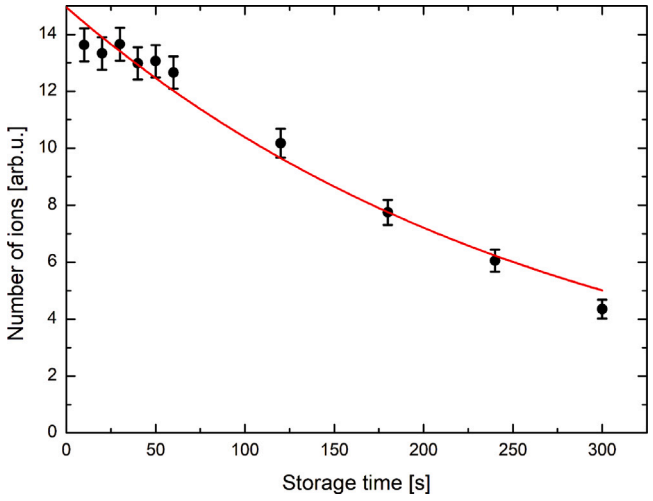

Fig. 10. Example results of a storage time test of the trap. The data have been averaged from 4 separate runs. The error bars correspond to one standard deviation. The number of ions is given in arbitrary units, one unit corresponding to approximately 1000 ions. Additionally, a fitting curve is presented, see the text for the details.

7. Source testing results

The tests were performed both for iodine and iodoform, in various time and voltage configurations. In both cases the results are qualitatively similar, so we present only selected datasets.

The loading run was performed with iodine molecules I_2. The presence of the molecular beam did not influence the vacuum level (10^{-9}mbar) inside the system, so we estimate the number density of molecules to be below 10^{14} m^{-3}. The ion energy was set to be 96 eV, and the cone of the channeltron was kept at 249 V, resulting in 345 eV kinetic energy of ions at the detector. The electron energy was set at 150 eV, resulting in 54 eV effective collision energy inside the trap.

In the following ion accumulation test, the ions were loaded for a given period of time. The electron gun was then switched off by turning off the filament heating. After next 10 s, the ions were released towards the detector and counted. The experiment was repeated 5 times for each loading time. The results are presented in Fig. 9.

The number of ions is given in arbitrary units, since exact determination of the detection efficiency is not possible. One unit corresponds to about 1000 ions. We note that the saturation in this particular test is reached at about 14 000 ions. In other tests, for example at higher number densities, we were able to reach up to 300 000 ions, and we expect to be able to improve this number by at least one order of magnitude in the future.

The experimental data were fitted with the function corresponding to the solution of Eq. (12):

$$N(t) = N_s\left(1 - \exp\left(-\frac{t}{\tau}\right)\right) \tag{15}$$

where N_s is the saturation number and τ is the characteristic time. From the fit we find $\tau = (40 \pm 6)$ s.

The second set of tests was the measurement of the storage time of the ions inside the trap. It was done under similar conditions, with modified procedure: for each run, the ion loading time was 60 s, and the waiting period before releasing the ions was varied. The results are presented in Fig. 10.

The data were fitted with the function:

$$N(t) = N_0 \exp\left(-\frac{t}{\tau_0}\right) \tag{16}$$

where N_0 is the initial number of ions trapped and τ_0 is the characteristic time. From the fit we obtain $\tau_0 = (274 \pm 19)$ s.

Both test results are consistent with Eq. (14). They lead to the conclusion that in this particular case: $\beta = (3.65 \pm 0.26) \cdot 10^{-3}$ s^{-1}, and $\frac{I}{e}\frac{\varsigma(E)}{S} = (21 \pm 5) \cdot 10^{-3}$ s^{-1}, which is consistent with the values assumed in Section 3.

Other measurement series lead to similar results, with saturation numbers and characteristic times depending on the conditions of particular experimental runs (beam intensities, energies, etc.)

8. Summary and future studies

To summarize, we designed, constructed and tested a long-lasting source of low-energy atomic anions of iodine, based on a Paul trap, using electron dissociative attachment to create the anions. The source provides repeatable pulses of anions, consisting of up to one million particles. The system is flexible with the choice of molecules to be used for ion production.

The studies will be continued to determine optimum conditions of use of the source combined with larger devices, such as the AEgIS apparatus at CERN. Also, cross sections for ion formation may be deduced from the analysis of subsequent tests of the device, providing new insight to the understanding of electron dissociative attachment experimental studies.

The device may be applied to produce other species of anions by replacing the iodine container with other molecular substances, such as other halogens or more complex molecules, including organic ones.

An interesting challenge would be the production of anions of atoms not forming molecules, for example metals. Such anions might be obtained via charge-transfer collisions of atoms with previously prepared anions. As an example let us consider the Cs^- anion. It may be produced in a reaction:

$$Cs + I^- \longrightarrow Cs^- + I \tag{17}$$

Since the electron affinity of iodine is 3.06 eV (Pelaez et al., 2009) and 0.47 eV (Navarrete et al., 2024) in the case of caesium, the threshold for the collision energy here is the difference of the affinities, equal to 2.59 eV. Heating the anion ensembles to such energies in the trapping potential is not a very challenging issue. Similar processes to Eq. (17) are possible for other species, with energy thresholds of the same order of few eV, which may finally allow to obtain a broad variety of possible anions.

CRediT authorship contribution statement

Ł. Kłosowski: Conceptualization, Formal analysis, Methodology, Software, Supervision, Writing – original draft, Writing – review & editing, Data curation, Funding acquisition, Investigation. **M. Piwiński:** Conceptualization, Investigation, Methodology, Project administration, Validation, Writing – original draft, Writing – review & editing, Data curation, Supervision, Funding acquisition. **A. Linek:** Data curation, Investigation, Writing – review & editing. **M. Grosbart:** Data curation, Writing – review & editing. **R. Ciuryło:** Investigation, Writing – review & editing. **M. Zawada:** Investigation, Writing – review & editing. **M. Teske:** Investigation, Writing – review & editing. **T. Sowiński:** Writing – review & editing. **S. Alfaro Campos:** Writing – review & editing. **M. Auzins:** Writing – review & editing. **D. Bhanushali:** Writing – review & editing. **A. Bhartia:** Writing – review & editing. **M. Berghold:** Writing – review & editing. **R.S. Brusa:** Writing – review & editing. **K. Calik:** Writing – review & editing. **A. Camper:** Writing – review & editing. **R. Caravita:** Conceptualization, Methodology, Writing – review & editing. **F. Castelli:** Writing – review & editing. **G. Cerchiari:** Writing – review & editing. **S. Chandran:** Writing – review & editing. **A. Chehaimi:** Writing – review & editing. **S. Choudapurkar:** Writing – review & editing. **P. Conte:** Writing – review & editing. **G. Consolati:** Writing – review & editing. **M. Doser:** Conceptualization, Writing – review & editing. **R. Ferguson:** Writing – review & editing. **M. Germann:** Writing – review & editing. **A. Giszczak:** Writing – review & editing. **L.T. Glöggler:** Writing – review & editing. **Ł. Graczykowski:** Writing – review & editing. **F. Guatieri:** Writing – review & editing. **F.P. Gustafsson:** Writing – review & editing. **S. Haider:** Writing – review & editing. **S. Huck:** Writing – review & editing. **C. Hugenschmidt:** Writing – review & editing. **M. Jakubowska:** Writing – review & editing. **M.A. Janik:** Writing – review & editing. **G. Kasprowicz:** Writing – review & editing. **K. Kempny:** Writing – review & editing. **G. Khatri:** Writing – review & editing. **A. Kisiel:** Writing – review & editing. **G. Kornakov:** Writing – review & editing. **V. Krumins:** Writing – review & editing. **L. Lappo:** Writing – review & editing. **S. Mariazzi:** Writing – review & editing. **P. Moskal:** Writing – review & editing. **M. Münster:** Writing – review & editing. **P. Pandey:** Writing – review & editing. **D. Pecak:** Writing – review & editing. **L. Penasa:** Writing – review & editing. **F. Prelz:** Writing – review & editing. **T. Rauschendorfer:** Writing – review & editing. **B.S. Rawat:** Writing – review & editing. **B. Rienäcker:** Writing – review & editing. **V. Rodin:** Writing – review & editing. **H. Sandaker:** Writing – review & editing. **S. Sharma:** Writing – review & editing. **E. Teberga:** Writing – review & editing. **M. Tockner:** Writing – review & editing. **M. Volponi:** Writing – review & editing. **C.P. Welsch:** Writing – review & editing. **J. Zieliński:** Writing – review & editing. **N. Zurlo:** Writing – review & editing.

Declaration of competing interest

The authors declare that they have no known competing financial interests or personal relationships that could have appeared to influence the work reported in this paper.

Acknowledgments

We thank B. Bergmann, P. Burian, S. Pospisil, P. Smolyanskiy and V. Petracek for financial support. Istituto Nazionale di Fisica Nucleare; the CERN Fellowship programme and the CERN Doctoral student programme; the EPSRC of UK Grant No. EP/X014851/1; Research Council of Norway under Grant Agreement No. 303337 and NorCC; CERN-NTNU doctoral program; the Research University – Excellence Initiative of Warsaw University of Technology via the strategic funds of the Priority Research Centre of High Energy Physics and Experimental Techniques; the IDUB POSTDOC programme; the SciMat and qLife Priority Research Areas budget under the program Excellence Initiative – Research University at Jagiellonian University; the Polish National Science Centre under Agreements No. 2022/45/B/ST2/02029, and No. 2022/46/E/ST2/00255, and No. 2023/50/E/ST2/00574, and by the Polish Ministry of Education and Science under Agreement No. 2022/WK/06; Wolfgang Gentner Programme of the German Federal Ministry of Education and Research (Grant No. 13E18CHA); the European Social Fund within the framework of realizing the project, in support of intersectoral mobility and quality enhancement of research teams at Czech Technical University in Prague (Grant No. CZ.1.07/2.3.00/30.0034).

Data availability

Data will be made available on request.

References

Andersen, T., 2004. Atomic negative ions: structure, dynamics and collisions. Phys. Rep. 394 (4), 157–313. http://dx.doi.org/10.1016/j.physrep.2004.01.001, URL https://www.sciencedirect.com/science/article/pii/S0370157304000316.

Bacal, M., Sasao, M., Wada, M., 2021. Negative ion sources. J. Appl. Phys. 129 (22), 221101. http://dx.doi.org/10.1063/5.0049289, URL http://arxiv.org/abs/https://pubs.aip.org/aip/jap/article-pdf/doi/10.1063/5.0049289/19890064/221101_1_5.0049289.pdf.

Bardsley, J.N., Mandl, F., 1968. Resonant scattering of electrons by molecules. Rep. Progr. Phys. 31 (2), 471. http://dx.doi.org/10.1088/0034-4885/31/2/302.

Barrow, R., Broyd, D., Pederson, L., Yee, K., 1973. The dissociation energies of gaseous Br2 and I2. Chem. Phys. Lett. 18 (3), 357–358. http://dx.doi.org/10.1016/0009-2614(73)80189-7, URL https://www.sciencedirect.com/science/article/pii/0009261473801897.

Cerchiari, G., Erlewein, S., Yzombard, P., Zimmermann, M., Kellerbauer, A., 2019. Capture of an external anion beam into a linear paul trap. J. Phys. B: At. Mol. Opt. Phys. 52 (15), 155003. http://dx.doi.org/10.1088/1361-6455/ab0089.

Deiglmayr, J., Göritz, A., Best, T., Weidemüller, M., Wester, R., 2012. Reactive collisions of trapped anions with ultracold atoms. Phys. Rev. A 86, 043438. http://dx.doi.org/10.1103/PhysRevA.86.043438, URL https://link.aps.org/doi/10.1103/PhysRevA.86.043438.

Esteves, B., Blondel, C., Chabert, P., Drag, C., 2023. Two-photon absorption laser induced fluorescence (talif) detection of atomic iodine in low-temperature plasmas and a revision of the energy levels of I I. J. Phys. B: At. Mol. Opt. Phys. 56 (5), 055002. http://dx.doi.org/10.1088/1361-6455/acb7b6.

Fabrikant, I.I., Eden, S., Mason, N.J., Fedor, J., 2017. Chapter nine - recent progress in dissociative electron attachment: From diatomics to biomolecules. In: Advances In Atomic, Molecular, and Optical Physics, vol. 66, Academic Press, pp. 545–657. http://dx.doi.org/10.1016/bs.aamop.2017.02.002, URL https://www.sciencedirect.com/science/article/pii/S1049250X17300034.

Frost, D.C., McDowell, C.A., 1960. The ionization and dissociation of some halogen molecules by electron impact. Can. J. Chem. 38 (3), 407–420. http://dx.doi.org/10.1139/v60-057.

Gulde, S., Rotter, D., Barton, P., Schmidt-Kaler, F., Blatt, R., Hogervorst, W., 2001. Simple and efficient photo-ionization loading of ions for precision ion-trapping experiments. Appl. Phys. B 73, 861–863.

Hartmann, J., 2000. Exotic Atoms. AccessScience, http://dx.doi.org/10.1036/1097-8542.YB000560, URL https://www.accessscience.com/content/article/aYB000560.

John Wiley and Sons, Ltd, 2016. Runge–Kutta Methods. pp. 143–331. http://dx.doi.org/10.1002/9781119121534.ch3, Ch. 3. http://arxiv.org/abs/https://onlinelibrary.wiley.com/doi/pdf/10.1002/9781119121534.ch3. URL https://onlinelibrary.wiley.com/doi/abs/10.1002/9781119121534.ch3.

Kjaergaard, N., Hornekaer, L., Thommesen, A.M., Videsen, Z., Drewsen, M., 2000. Isotope selective loading of an ion trap using resonance-enhanced two-photon ionization. Appl. Phys. B: Lasers Opt. 71, 207–210.

Kłosowski, Ł., Piwiński, M., Wójtewicz, S., Lisak, D., 2018. Measurement of electron-calcium ionization integral cross section using an ion trap with a low-energy, pulsed electron gun. J. Electron Spectrosc. Relat. Phenom. 228, 13–19. http://dx.doi.org/10.1016/j.elspec.2018.08.002, URL http://www.sciencedirect.com/science/article/pii/S0368204818300963.

Lakhmanskaya, O., Simpson, M., Wester, R., 2020. Vibrational overtone spectroscopy of cold trapped hydroxyl anions. Phys. Rev. A 102, 012809. http://dx.doi.org/10.1103/PhysRevA.102.012809, URL https://link.aps.org/doi/10.1103/PhysRevA.102.012809.

Major, F.G., Gheorghe, V.N., Werth, G., 2005. Charged particle traps. In: Physics and Techniques of Charged Particle Field Confinement. Springer.

Mant, B.P., Gianturco, F.A., Wester, R., Gonzalez-Sanchez, L., Yurtsever, E., 2020. Thermalisation of C2- with noble gases in cold ion traps. Int. J. Mass Spectrom. 457, 116426. http://dx.doi.org/10.1016/j.ijms.2020.116426, URL https://www.sciencedirect.com/science/article/pii/S1387380620303493.

Middleton, R., 1983. A versatile high intensity negative ion source. Nucl. Instrum. Methods Phys. Res. 214 (2), 139–150. http://dx.doi.org/10.1016/0167-5087(83)90580-X, URL https://www.sciencedirect.com/science/article/pii/016750878390580X.

Navarrete, J.E. Navarro, Nichols, M., Ringvall-Moberg, A., Welander, J., Lu, D., Leimbach, D., Kristiansson, M.K., Eklund, G., Raveesh, M., Chulkov, R., Zhaunerchyk, V., Hanstorp, D., 2024. High-resolution measurement of the electron affinity of cesium. Phys. Rev. A 109, 022812. http://dx.doi.org/10.1103/PhysRevA.109.022812, URL https://link.aps.org/doi/10.1103/PhysRevA.109.022812.

Otto, R., von Zastrow, A., Best, T., Wester, R., 2013. Internal state thermometry of cold trapped molecular anions. Phys. Chem. Chem. Phys. 15, 612–618. http://dx.doi.org/10.1039/C2CP43186F.

Pelaez, R.J., Blondel, C., Delsart, C., Drag, C., 2009. Pulsed photodetachment microscopy and the electron affinity of iodine. J. Phys. B: At. Mol. Opt. Phys. 42 (12), 125001. http://dx.doi.org/10.1088/0953-4075/42/12/125001.

Stull, D.R., 1947. Vapor pressure of pure substances. Org. Inorg. Compd. Ind. Eng. Chem. 39 (4), 517–550. http://dx.doi.org/10.1021/ie50448a022.

Vretenar, M., Bauche, J., Baudrenghien, P., Body, Y., Brunner, O., Buzio, M., Calviani, M., DosSantos, N., Fuchs, J.F., Funken, A., Gerigk, F., Hansen, J., Kozsar, I., Lallement, J.B., Lettry, J., Lombardi, A., Lopez-Hernandez, L.A., Martin, C., Mathot, S., Mompo, R., Nisbet, D., Puccio, B., Raich, U., Ramberger, S., Roncarolo, F., Rossi, C., Scrivens, R., Vollaire, J., Zickler, T., 2020. Linac4 design report, CERN yellow reports: Monographs. http://dx.doi.org/10.23731/CYRM-2020-006.

Werth, G., Gheorghe, V.N., Major, F.G., 2009. Charged particle traps II. In: Applications. Springer.

Yadav, H., Vinodkumar, M., Limbachiya, C., Vinodkumar, P., Mason, N., 2020. Low energy electron interactions with iodine molecule (I2). J. Quant. Spectrosc. Radiat. Transfer 250, 107035. http://dx.doi.org/10.1016/j.jqsrt.2020.107035, URL https://www.sciencedirect.com/science/article/pii/S0022407319306107.

Zatsarinny, O., Bartschat, K., Garcia, G., Blanco, F., Hargreaves, L., Jones, D., Murrie, R., Brunton, J., Brunger, M., Hoshino, M., Buckman, S., 2011. Electron-collision cross sections for iodine. Phys. Rev. A 83, 042702. http://dx.doi.org/10.1103/PhysRevA.83.042702, URL https://link.aps.org/doi/10.1103/PhysRevA.83.042702.